ELSEVIER

Preparation of polypyrrole microstructures by direct electrochemical oxidation of pyrrole in an aqueous solution of camphorsulfonic acid

Liangti Qu, Gaoquan Shi *, Jinying Yuan, Gaoyi Han, Feng'en Chen

Department of Chemistry, Tsinghua University, Beijing 100084, PR China

Received 11 February 2003; received in revised form 7 July 2003; accepted 15 July 2003

Abstract

Polypyrrole microstructures with morphology like bowls, cups and bottles have been generated electrochemically by direct oxidation of pyrrole in an aqueous solution of camphorsulfonic acid. The well-ordered microstructures stand upright on the working electrode surface in a high density. Their morphological features can be easily controlled by changing the electrochemical polymerization conditions and the results have good reproducibility. The growth process of microstructures was studied by scanning electron microscopy and optical microscopy. Based on the experimental observations, a self-assembled gas bubble template mechanism was postulated.
© 2003 Elsevier B.V. All rights reserved.

Keywords: Polypyrrole; Microstructure; Electrochemical oxidation

1. Introduction

Intrinsically conducting polymers (ICPs) are a new generation of polymers, because they cover the full range from insulator to metal and retain the attractive mechanical properties as well as the processing advantages of polymers [1–3]. Therefore, conducting polymers have been extensively explored as alternatives to metals or inorganic semiconductors in the fabrication of microelectronic, optoelectronic, and microelectromechanical devices [4–6]. Most of the applications in microsystems require the formation of patterned microstructures of conducting polymers. Up to now, a number of techniques have been developed for microstructuring ICPs, such as laser-induced polymerisation, laser ablation, polymerisation on a prestructured substrate and soft lithography [7–10]. Microtubules and microspheres of ICPs can be prepared via a template or a template-free route [11–19]. Although aligned microstructures based on the features of the template can be

produced, the template-guided synthesis technique is expensive and the solid template limits the size of the material. Therefore, synthesis of aligned ICP microstructures with the desired morphology without using a solid template has been a challenge for a long time.

On the other hand, polypyrrole (PPy) is an intrinsically conducting polymer with various interesting properties such as high conductivity, good thermal and environmental stability, and biocompatibility [20]. Microstructured polypyrrole is useful for fabricating microdevices including reactors, actuators and sensors [14,21–23].

In this paper, we report a novel electrochemical route to prepare well-aligned three-dimensional polypyrrole (PPy) microstructures. The formations of the unusual microstructures were due to the fact that the self-assembled gas bubbles on the working electrode acted as the template.

2. Experimental

(+)- and (−)-Camphorsulfonic acids (Fluka, Japan) were used as received and pyrrole (Chinese Army

---

Medical Institute, Beijing, China) was used after distillation. The growth of polypyrrole (PPy) microstructures was carried out at room temperature in a one-compartment cell (5 cm³) (except as mentioned otherwise in the text) by the use of a Model 283 potentiostat–galvanostat (EG&G Princeton Applied Research) under computer control. The working and counter electrodes were two stainless steel sheets (AISI 321) with surface areas of 0.5 cm² each and a face to face spacing of 0.5 cm. All potentials were referred to a saturated calomel electrode (SCE). The solutions were deaerated by a dry nitrogen stream and maintained at a light overpressure during the experiments. Before growing PPy microstructures, the solution was pretreated by cyclic voltammetric scanning over the potential range of 0–1.4 V at a scan rate of 20 mV/s for 2 cycles to produce enough suspended gas bubbles (accompanied by the polymerization of pyrrole on the working electrode). The typical electrolyte was an aqueous solution of 0.5 M pyrrole and 0.6 M (+)- or (−)-camphorsulfonic acid.

The infrared spectra were obtained by the use of a Spectrum GX FT-infrared spectrometer (Perkin–Elmer) with KBr pellets. Raman spectra were recorded by using a RM 2000 microscopic confocal Raman spectrometer (Renishaw PLC, England) employing a 633 nm laser beam. The optical microscopic images of gas bubbles assembled on the electrode surface were taken by the use of a Leica DMLM (Germany) microscope and connected to a CCD camera. The morphology of the microstructures was studied using a KYKY2800 scanning electron microscope (Beijing Scientific Instrument Company, Beijing, China) after sputter-coating the samples with gold. Dynamic light scattering tests were carried out on a DLS-700 dynamic light scattering spectrophotometer with a 632.8 nm light source (Stsuka, Japan) at room temperature. The specific surface areas of the microstructures were determined by the nitrogen absorption BET method (ASAP2010, Micromeritics).

3. Results and discussion

3.1. Morphology

Fig. 1 shows typical scanning electron microscopic (SEM) images of PPy microstructures obtained by electrolysis of 0.5 M pyrrole in 0.6 M (−)-camphorsulfonic acid ((−)-CSA) aqueous solution at different applied potentials for 240 s each. It is clear from this figure that the microstructures stand upright on the electrode surface and align fairly well in a high density. Micro-cups (Fig. 1(A)) with a diameter of ca. 60–80 μm and height of ca. 100 μm were formed at a low applied potential of 0.8 V. With the increase of applied potential, the height of the microstructures increased while their diameter changed only a little. Microtubules
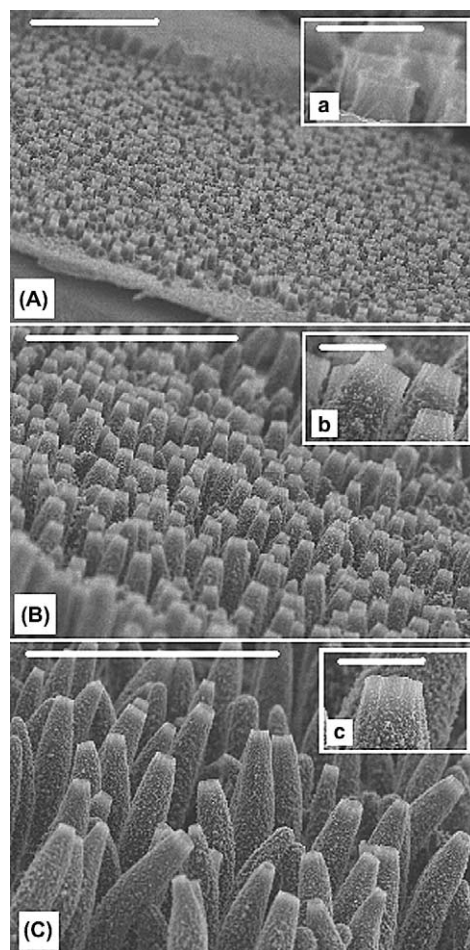

Fig. 1. SEM images of PPy microstructures obtained by electrolysis of 0.5 M Py in an aqueous solution of 0.6 M (−)-CSA at different applied potentials (A, 0.8 V; B, 1.0 V; C, 1.2 V) for 240 s each. Scale bars: A, B and C, 1 mm; a, b and c, 100 μm.

about 1 mm long were obtained at 1.2 V as shown in Fig. 1(C).

Polypyrrole microstructures also can be generated and controlled by the cyclic voltammetric (CV) scanning technique. Figs. 2(A–D) illustrate the SEM images of microstructures grown in the aqueous medium of 0.5 M pyrrole and 0.6 M (−)-CSA by CV scanning in the potential range of 0–1.2 V at 20 mV/s for different cycles. Potential scanning for 1 cycle generated micro-bowls of ca. 50 μm diameter and ca. 40 μm height (Fig. 2(A)). The walls of the micro-bowls are smooth and thin. As the cyclic potential scan number increased to 2, the microstructures grew higher (ca. 100 μm) and their walls became rougher and thicker (Fig. 2(B)). Furthermore, a neck appeared between the two parts formed in the first and the second scan cycles. Further experiments confirmed (as shown in Figs. 2(C) and (D)) that the microstructures grew from bottom to top and that the number of annular parts in a single microstructure was consistent with that of the number of CV cycles. In addition, the potential scan rate could also affect the
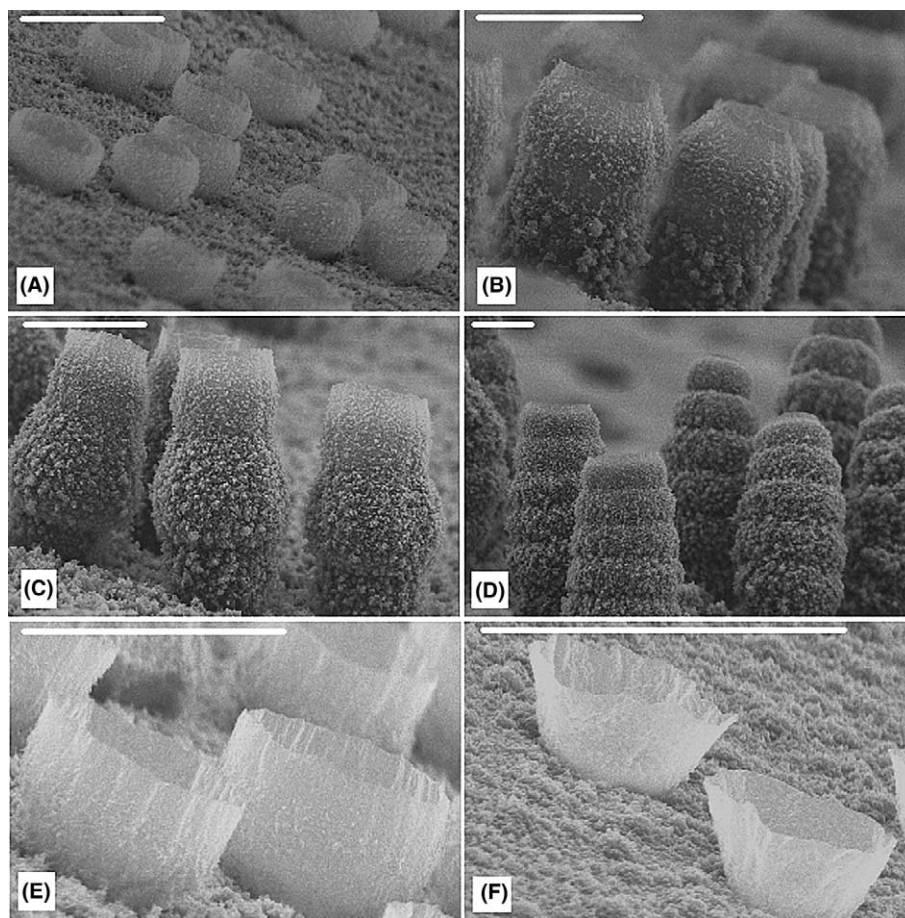
Fig. 2. SEM images of the microstructures generated by voltammetric scanning at a scan rate of 20 mV/s in the potential range of 0–1.2 V for different cycles (A, 1; B, 2; C, 3; D, 7) or at different scan rates (E, 50 mV/s; F, 150 mV/s) for 3 cycles. The electrolyte is an aqueous solution of 0.5 M pyrrole and 0.6 M (−)-camphorsulfonic acid. Scale bars: 100 μm.

morphology of the microstructures. As shown in Figs. 2(E) and (F), the micro-bowls obtained at a scan rate of 50 mV/s (Fig. 2(E)) are larger than those prepared at a scan rate of 150 mV/s (Fig. 2(F)). In contrast to Fig. 2(C), there was no neck formed on the bowls. This is mainly due to the fact that that a high potential scan rate results in a high PPy growth rate and a short time interval between two neighboring cycles.

Fig. 3 shows the SEM images of the microstructures produced by one CV scan cycle in different potential ranges. The micro-bowls obtained in the narrow potential range of 0–0.8 V (Fig. 3(A)) had a diameter of 50 μm. From Figs. 3(B)–(D), with the increase of the upper switching potential, the shapes of the microstructures changed from micro-bowls (Fig. 3(B)) to micro-barrels (Fig. 3(C)), and to micro-bottles (Fig. 3(D)), accompanied with the decrease of their diameters from ca. 80 μm (Fig. 3(B)) to ca. 30 μm (Fig. 3(D)).

Aligned PPy microstructures also can be obtained by other electrochemical techniques. Fig. 4 illustrates the microstructures prepared galvanostatically at different current densities. It is clear from this figure, with the increase of current density, that the heights of the microstructures increase and their shapes change from micro-bowls (Fig. 4(A)) to micro-barrels (Fig. 4(D)). The microstructures can even be generated by linear potential scanning. As shown in Fig. 5, micro-bowls with different morphologies were prepared by linear potential scanning at 20 mV/s in different potential ranges.

Different substrates such as platinum, p- or n-type silicon, indium–tin-oxide (ITO)-coated glass and gold-coated stainless steel electrodes can be used to grow PPy microstructures. The crock-like microstructures (Fig. 6(A)) were generated on the surface of the platinum electrode by two CV scan cycles over 0–1.2 V. The "goblets" (Fig. 6(B)) were obtained by electrolysis at 1.2 V for 60 s and successively at 1.0 V for 120 s on a p-silicon substrate with a resistance of 10^{-3} Ω cm. The microstructures grown on indium–tin-oxide coated glass and gold-coated stainless steel surfaces are shown in Figs. 6(C) and (D), respectively.

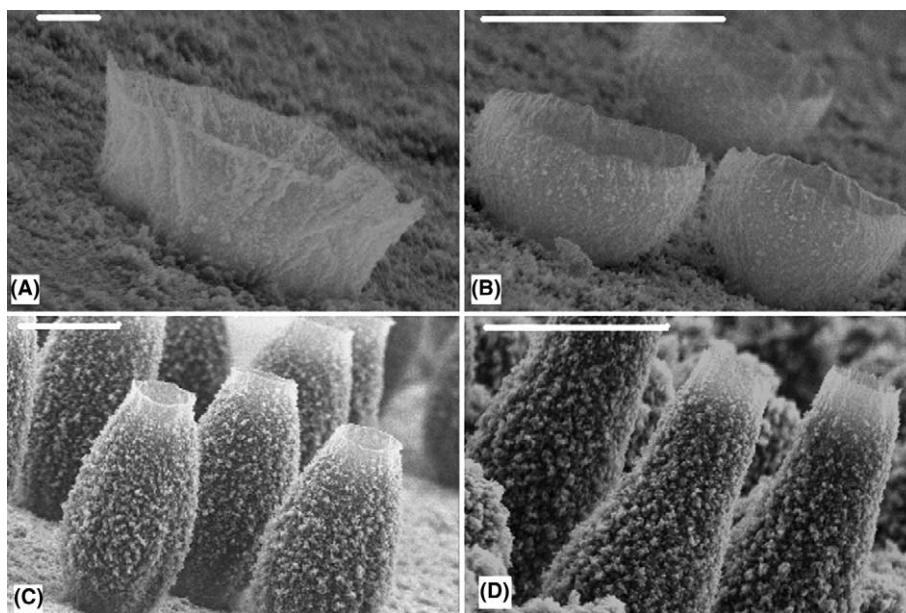Whether (+)- or (−)-camphorsulfonic acid was used, as long as the electrolysis conditions were the same,

Fig. 3. SEM images of the microstructures produced by 1 CV scan cycle at a scan rate of 20 mV/s in different potential ranges (A, 0–0.8 V; B, 0–1.0 V; C, 0–1.2 V; D, 0–1.4 V) in a solution of 0.5 M pyrrole and 0.6 M (−)-CSA. Scale bars: A, 10 μm; B–D, 100 μm.

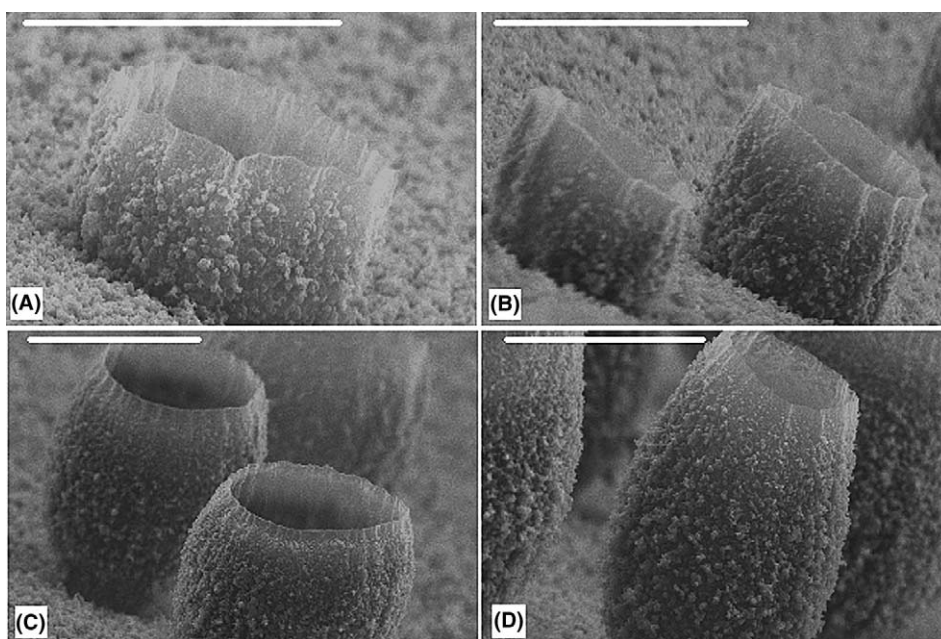

Fig. 4. SEM images of the microstructures prepared galvanostatically for 60 s at different current densities (A, 20 mA/cm^2; B, 40 mA/cm^2; C, 55 mA/cm^2; D, 70 mA/cm^2) in a solution of 0.5 M pyrrole and 0.6 M (−)-CSA. Scale bars: 100 μm.

microstructures with similar morphological features were observed. Furthermore, microstructures with similar morphologies also can be formed in other electrolytes such as aqueous solutions of naphthalenesulfonic acid, sodium dodecylbenzenesulfonate and polystyrenesulfonic acid. The morphology of PPy microstructures depends only on the electrolysis conditions, and the shape and size of the microstructures can be easily controlled by changing the electrochemical conditions.

3.2. Raman and infrared spectra characterization

The 633 nm excited microscopic Raman spectra (the laser spots focused on the inside and outside surfaces of the walls gave spectra with similar features) of the mi-
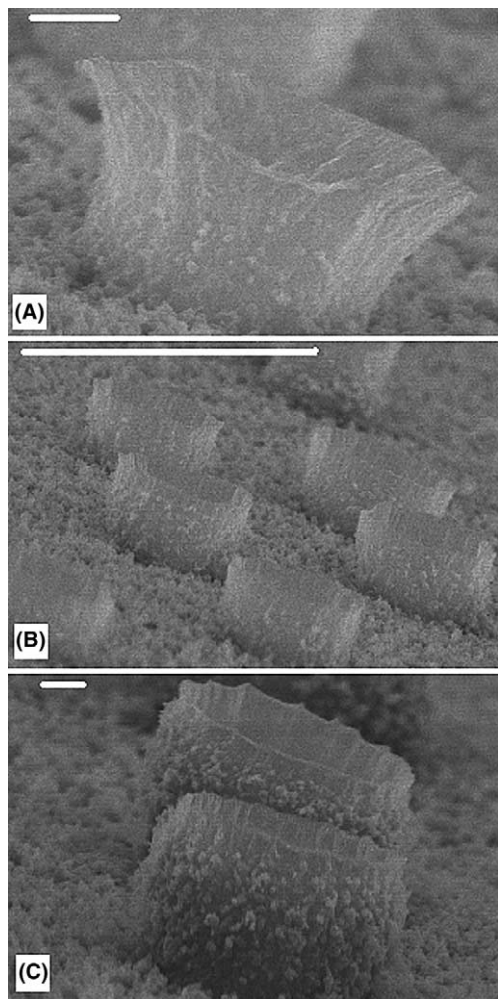
Fig. 5. SEM images of the microstructures obtained by linear potential scanning at 20 mV/s from 1.2 V (A), 1.4 V (B), 1.6 V (C) to 0 V in a solution of 0.5 M pyrrole and 0.6 M (−)-CSA. Scale bars: A, C, 10 μm; B, 100 μm.

crostructures (Fig. 7(A)) showed strong bands at ca. 1370 and 1085 cm^{-1} which were attributed to the ring stretching and the N–H in-plane deformation of the oxidized (doped) species, respectively [24,25]. The Raman band at ca. 1600 cm^{-1} represents the backbone stretching mode of C=C bonds. The FT-infrared spectra of the microstructures (Fig. 7(B)) are similar to those of PPy obtained by other methods [26–28]. Two bands at 1035 and 1735 cm^{-1} are attributed, respectively, to the –SO$_3^-$ group and carbonyl group of the camphorsulfonic acid. The strong bands near 2800 and 2900 cm^{-1} are assigned to the CH$_3$ and CH$_2$ groups of camphorsulfonic acid. These results indicate that the PPy microstructures were doped by chiral (+)- or (−)-camphorsulfonic acid. The infrared spectrum of the same sample in the dedoped state showed no bands of the carboxyl group at around 1700 cm^{-1} (Fig. 7(C)), indicating that the polymer was not overoxidized in the growth process. The conductivity of the PPy film with

microstructures obtained at 0.8 V for 360 s is 3.9 S cm^{-1} and that prepared at 1.4 V for 360 s is 0.29 S cm^{-1}. These values are close to those reported previously for CSA doped PPy films [29].

3.3. Electrochemical properties

The cyclic voltammogram of the PPy film with micro-cups (4.1 C cm^{-2}) in an aqueous solution of 0.6 M (+)-CSA or 0.6 M (−)-CSA (Fig. 8) showed a pair of strong and broad oxidation and reduction waves at ca. 0.6 and −0.3 V, respectively. This is mainly due to the fact that the polypyrrole films with microstructures have a much larger surface area than that of a normal film, which results in much higher film/electrolyte double-layer capacitive charges. For example, the specific surface area of the PPy film with micro-cups grown for 3.4 C cm^{-2} (measured by nitrogen absorption) is about 74 times that of the flat PPy film (rms roughness = 110 nm) grown for the same charge density. Therefore, the PPy films with microstructures may have potential applications in fabrication of high-quality microelectronics such as capacitors and sensors.

3.4. Formation mechanism

Dynamic light scattering tests showed that the micelles in the aqueous solution of 0.5 M pyrrole and 0.6 M (+)- or (−)-CSA had an average diameter of 40 or 23 nm, respectively. These values are far smaller than the size of the PPy microstructures (∼50 μm). Therefore, it is illogical to explain the formation of the microstructures by a micelle template mechanism. On the other hand, it was observed (by the naked eye) that a large amount of hydrogen gas was released from the counter electrode during the electrolysis process. This is mainly due to the following reactions

$$+ 2nH^+ \quad \text{(Anode)}$$

$$2n\,H^+ + 2ne^- \longrightarrow nH_2 \uparrow \quad \text{(Cathode)}$$
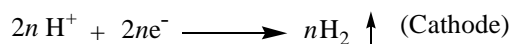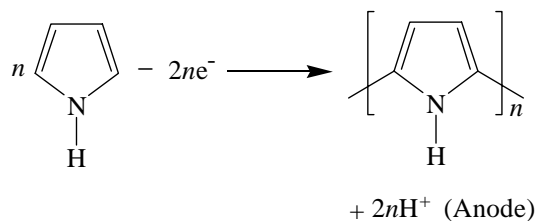
While many publications showed only the half reaction at the anode, the cathode reaction can be derived from the charge and mass balances of the whole redox reactions. In the aqueous solution of (+)- or (−)-CSA (a typical surfactant), small gas bubbles were enwrapped
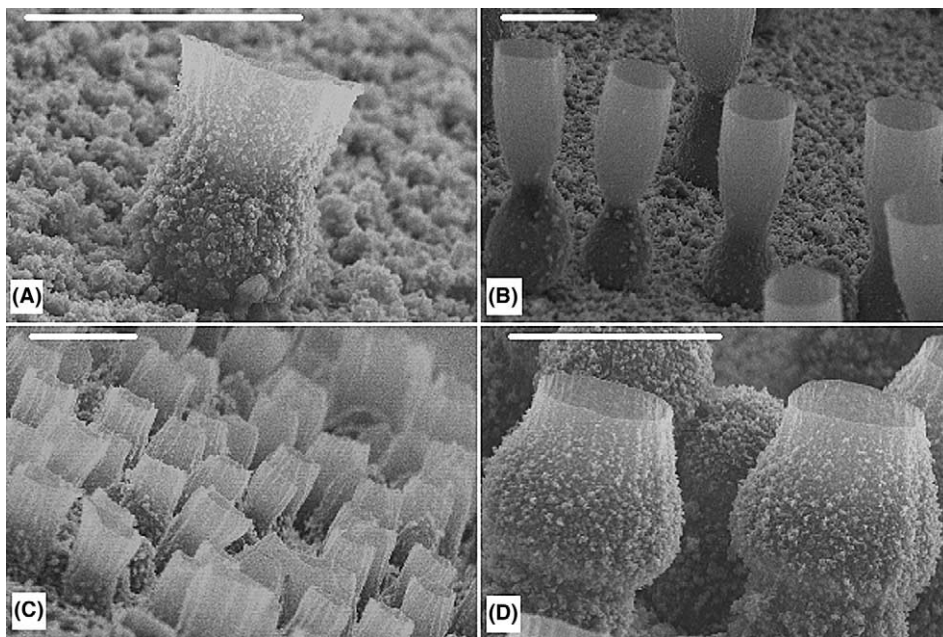
Fig. 6. SEM images of microstructures grown on different electrode surfaces (A, platinum; B, silicon; C, indium–tin-oxide (ITO)-coated glass; D, gold-coated stainless steel) in an aqueous solution of 0.5 M pyrrole and 0.6 M (−)-CSA. A and D were prepared by 2 cyclic voltammetric scan cycles in the potential range of 0–1.2 V at a scan rate of 20 mV/s; B was formed by electrolysis at 1.2 V for 60 s and successively 1.0 V for 120 s; C was generated potentiostatically at a potential of 1.4 V for 240 s. Scale bars: 100 μm.
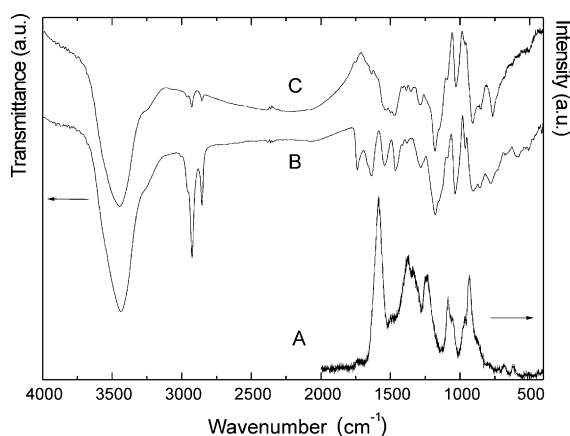

Fig. 7. Raman (A) and infrared spectra (B, C) of the microstructures obtained by 2 CV scan cycles in a potential range of 0–1.4 V in a solution of 0.5 M pyrrole and 0.6 M (+)- or (−)-CSA. (The samples of A and B were in the doped state and that of C was in the dedoped state.)

Fig. 8. Cyclic voltammogram of the PPy film with micro-cups (4.1 C cm^{-2}) in an aqueous solution of 0.6 M (+)-CSA (A) and (−)-CSA (B).

by the surfactants with negative charges and dispersed in the aqueous solution. As a positive potential was applied, the gas bubbles close to the anode were assembled on the surface of the working electrode under the function of the electric field. Fig. 9 shows the optical microscopic images of the surface of the working electrode during the course of potential scanning from 0 to 0.8 V. It is clear from this figure, that at 0.8 V, many gas bubbles were assembled on the electrode surface. The diameter of gas bubbles is about 50 μm which is comparative to the size of PPy microstructures formed ini-
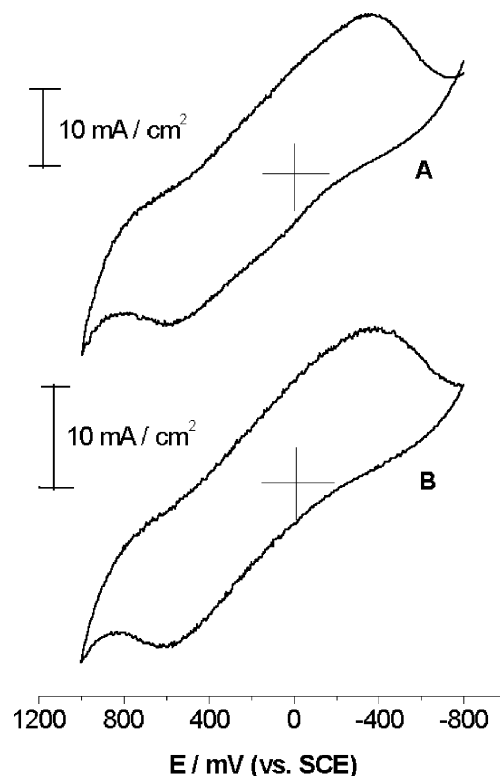
tially as shown in Figs. 2(A) and 3(A). The central parts of the microbubbles are transparent but their edges are obscure. The obscure parts can be considered to be due
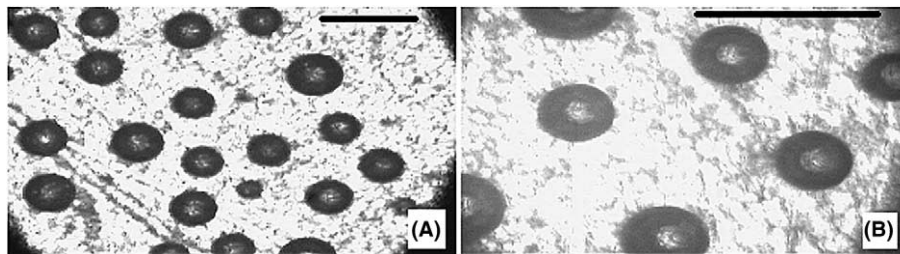
Fig. 9. Optical microscopic images of the gas bubbles assembled on the surface of the working electrode. Scale bars: 100 μm.

to the slight polymerisation of pyrrole surrounding the gas bubbles at about 0.8 V. This implies that the polymerisation was accompanied with gas bubble assembly. With a two-compartments cell for electrolysis (the working electrode separated from the counter electrode), the PPy microstructures could not be generated at a potential lower than 1.2 V. This is mainly because the gas bubbles produced at the counter electrode can-

not move to the working electrode surface. Therefore, it is reasonable to conclude that the growth of microstructures is due to the gas bubbles assembled on the working electrode surface acting as a template. Few microstructures were generated in the aqueous electrolyte without a surfactant. In organic media such as acetonitrile, microstructures also cannot be generated. In these systems, although H_2 gas was produced, the gas bubbles cannot be enwrapped by surfactant and dispersed in the medium or escape from the solution quickly. These results also strongly support the postulated mechanism described above.

On the other hand, it is known that the decomposition potential of acidic water is 1.23 V (vs. SCE) [30]. At potentials higher than this value, oxygen gas also can be produced on the working electrode. As a result, the microstructures of PPy can also be generated at relative high potentials even using a two-compartment cell for polymerisation (Fig. 10). This is due to the oxygen gas bubbles formed on the working electrode acting as the template. In conclusion, at relatively higher potentials (>1.23 V, vs. SCE) the growth of the microstructures in a one-compartment cell should be attributed to the combinative actions of the H_2 and O_2 gas bubbles formed at the counter and working electrodes, respectively. The "gas bubble" size and generation rate and the growth rate of PPy film surrounding the gas bubbles depend strongly on the experimental conditions. Thus, changing the electrolysis conditions can easily control the shape, size and diameter of the PPy microstructures.

Fig. 10. SEM images of microstructures formed by the oxygen gas bubble template. "A" was formed by 2 cyclic voltammetric scan cycles in the potential range of 0–1.4 V. "B" and "C" were obtained at applied potential of 1.5 and 1.2 V for 120 s each, respectively. The electrolyte was an aqueous solution of 0.5 M pyrrole and 0.6 M (−)-CSA. Scale bars: 100 μm.

4. Conclusions

Polypyrrole microstructures with very unusual morphology can be generated by electropolymerization of pyrrole in an aqueous solution of camphorsulfonic acid. The shape and size of the microstructures can be modulated electrochemically. The microstructures are made of PPy in the doped state. The PPy films with microstructures showed strong and broad redox waves in the electrolyte of aqueous (+)-or (−)-camphorsulfonic acid solution because of their large surface areas. The growth process of the microstructures has been studied and a self-assembled gas bubble template mechanism is put
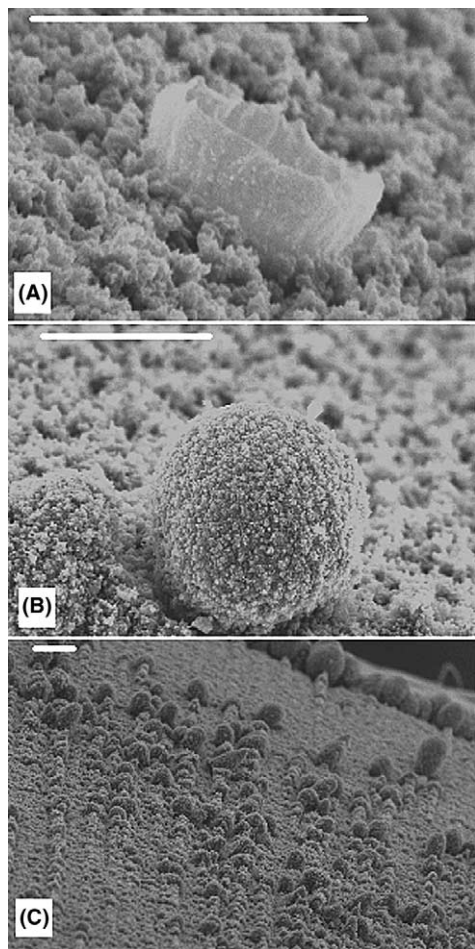
forward. In addition, the technology developed by this work can be extended to synthesize other materials with similar microstructures by changing the monomers and surfactants.

Acknowledgements

References

[1] A.J. Heeger, Rev. Mod. Phys. 73 (2001) 681.
[2] A.G. MacDiarmid, Synth. Met. 125 (2001) 11.
[3] T.A. Skotheim, R.L. Elsenbaumer, J.R. Reynolds, Handbook of Conjugated Polymers, second ed., Marcel Dekker, New York, 1998.
[4] J.W. Gardner, P.N. Bartlett, Sensors and Actuators A 51 (1995) 57.
[5] R.H. Baughman, Synth. Met. 78 (1996) 339.
[6] G. Horowitz, Adv. Mater. 10 (1998) 365.
[7] J.W. Schultze, T. Morgenstern, D. Schattka, S. Winkels, Electrochim. Acta 44 (1999) 1847.
[8] W.S. Beh, I.T. Kim, D. Qin, Y.N. Xia, G.M. Whitesides, Adv. Mater. 11 (1999) 1038.
[9] C. Decker, Proc. SPIE Int. Soc. Opt. 112 (1989) 1022.
[10] T. Lippert, A. Wokaun, Chimia 55 (2001) 783.
[11] V.M. Cepak, C.R. Martin, Chem. Mater. 11 (1999) 1363.
[12] S. Devito, C.R. Martin, Chem. Mater. 10 (1998) 1738.
[13] C.R. Martin, R.V. Parthasarathy, Adv. Mater. 7 (1995) 487.
[14] R.V. Parthasarathy, C.R. Martin, Nature 369 (1994) 298.
[15] Z.X. Wei, M.X. Wan, Adv. Mater. 14 (2002) 1314.
[16] Z.M. Zhang, Z.X. Wei, M.X. Wan, Macromolecules 35 (2002) 5937.
[17] K. Huang, M.X. Wan, Chem. Mater. 14 (2002) 3486.
[18] M.X. Fu, Y.F. Zhu, R.Q. Tan, G.Q. Shi, Adv. Mater. 13 (2001) 1874.
[19] M.X. Fu, F.E. Chen, J.X. Zhang, G.Q. Shi, J. Mater. Chem. 12 (2002) 2331.
[20] P. Bornier, S. Lefrant, G. Bidan (Eds.), Advances in Synthetic Metals, Elsevier, Amsterdam, 1999.
[21] N. Guernion, R.J. Ewen, K. Pihlainon, N.M. Ratcliffe, G.C. Teare, Synth. Met. 126 (2002) 301.
[22] E.W.H. Jager, E. Smela, O. Inganas, Science 290 (2000) 1540.
[23] E.W.H. Jager, O. Ingansa, I. Lundstrom, Science 288 (2000) 2335.
[24] Y.C. Liu, B.J. Hwang, W.J. Jian, R. Santhanan, Thin Solid Films 374 (2000) 85.
[25] J. Mikat, I. Orgzall, H.D. Hochheimer, Phys. Rev. B 65 (2002) 174202.
[26] Y.S. Yang, M.X. Wan, J. Mater. Chem. 11 (2001) 2022.
[27] F.I. Mathy, V.T. Truong, Synth. Met. 89 (1997) 103.
[28] B. Tian, G.J. Zerbi, Chem. Phys. 92 (1990) 3886.
[29] Y.Q. Shen, M.X. Wan, Synth. Met. 96 (1998) 127.
[30] N. Sakmeche, S. Aeiyach, J.J. Aaron, M. Jouini, J.C. Lacroix, P.C. Lacaze, Langmuir 15 (1999) 2566.